Inhibition of the Enhancement of Infection of Human Immunodeficiency Virus by Semen-Derived Enhancer of Virus Infection Using Amyloid-Targeting Polymeric Nanoparticles

Daniel A. Sheik,[†,§] Lauren Brooks,[‡,§] Kristen Frantzen,[‡] Stephen Dewhurst,[‡] and Jerry Yang*[,†]

[†]Department of Chemistry and Biochemistry, University of California, San Diego, 9500 Gilman Drive, La Jolla, California 92093-0358, United States and [‡]Department of Microbiology and Immunology, University of Rochester, Rochester, New York 14642, United States. [§]These authors (D.A.S. and L.B.) contributed equally.

ABSTRACT The semen-derived enhancer of virus infection (SEVI) is a natural amyloid material that has been shown to substantially increase viral attachment and infectivity of HIV in cells. We previously reported that synthetic monomeric and oligomeric amyloid-targeting molecules could form protein-resistive coatings on SEVI and inhibit SEVI- and semen-mediated enhancement of HIV infectivity. While oligomeric amyloid-binding compounds showed substantial improvement in apparent binding to SEVI compared to monomeric compounds, we observed only a modest correlation between apparent binding to SEVI and activity for reducing SEVI-mediated HIV infection. Here, we synthesized amyloid-binding polyacrylate-based polymers and polymeric nanoparticles of comparable size to HIV virus particles (~150 nm) to assess the effect of sterics on the inhibition of SEVI-mediated enhancement of HIV infectivity. We show that these polymeric materials exhibit excellent capability to reduce SEVI-mediated enhancement of HIV infection, with the nanoparticles exhibiting the greatest activity (IC_{50} value of ~4 μg/mL, or 59 nM based on polymer) of any SEVI-neutralizing agent reported to date. The results support that the improved activity of these nanomaterials is likely due to their increased size (diameters = 80–200 nm) compared to amyloid-targeting small molecules and that steric interactions may play as important a role as binding affinity in inhibiting viral infection mediated by SEVI amyloids. In contrast to the previously reported SEVI-neutralizing, amyloid-targeting molecules (which required concentrations at least 100-fold above the K_d to observe activity), the approximate 1:1 ratio of apparent K_d to IC_{50} for activity of these polymeric materials suggests the majority of polymer molecules that are bound to SEVI contribute to the inhibition of HIV infectivity enhanced by SEVI. Such size-related effects on physical inhibition of protein–protein interactions may open further opportunities for the use of targeted nanomaterials in disease intervention.

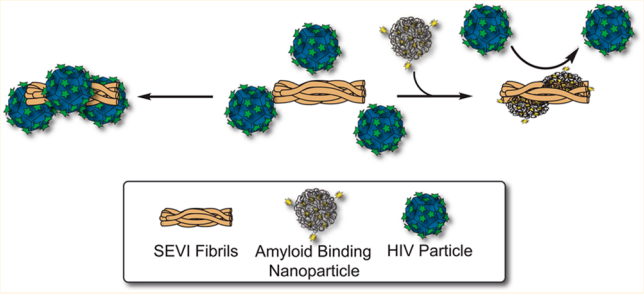

KEYWORDS: SEVI · HIV · polymer · acrylate · nanoparticles · steric inhibition

The most common mode for transmission of HIV is through sexual contact.[1] Recent studies have shown that several peptides found in high abundance in semen can form aggregated amyloid species capable of facilitating viral attachment and internalization in cells.[2−8] For instance, the amyloid form of a peptide derived from prostatic acid phosphatase, PAP248-286 (known as the semen-derived enhancer of virus infection or SEVI), has been reported to increase the rate of HIV infection by up to 400,000-fold, making this naturally abundant amyloid species a particularly attractive target for development of molecules that can reduce the spread of HIV.[2,5,9−14]

Previously, we reported that monomeric and oligomeric amyloid-targeting 6-methylbenzothiazole aniline (BTA) compounds could form protein-resistive coatings[15−19] on amyloids and could inhibit SEVI-mediated HIV infection.[20,21] We showed that while the monomeric BTA molecules were effective at inhibiting HIV infection, oligomeric versions of BTA exhibited improved activity for inhibiting SEVI-mediated HIV infection. These BTA

* Address correspondence to jerryyang@ucsd.edu.

Received for review November 25, 2014 and accepted January 25, 2015.

Published online January 26, 2015
10.1021/nn5067254

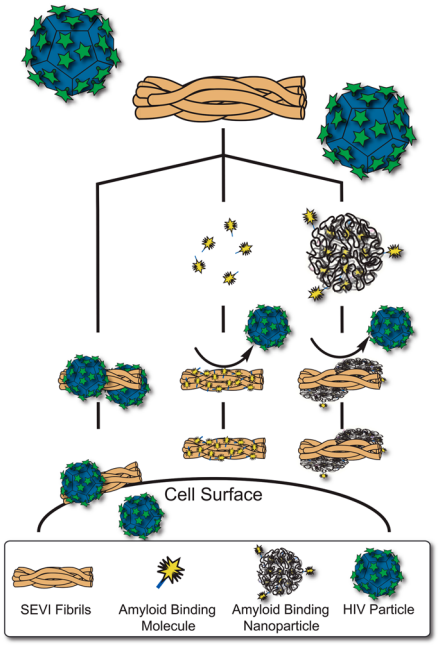

Figure 1. Illustration of the inhibition of binding of HIV virions and SEVI amyloid fibrils using amyloid-binding small molecules or amyloid-binding polymeric nanoparticles. Inhibiting HIV−SEVI interactions results in reduction of SEVI-enhanced HIV infection in cells.

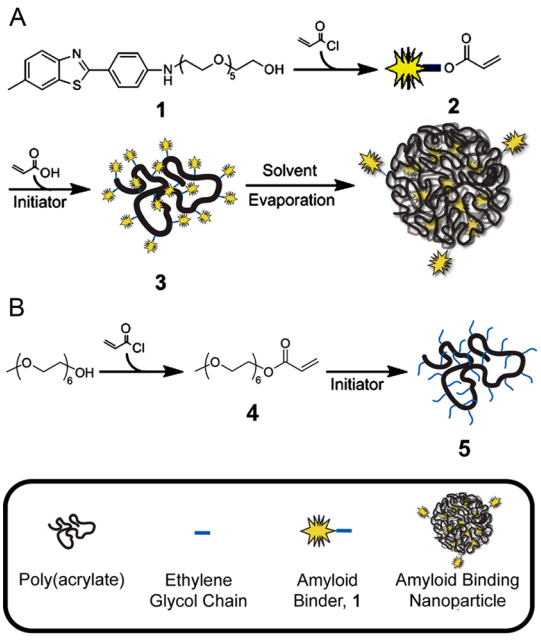

Figure 2. Scheme for the synthesis of BTA-containing polyacrylate-based polymer 3 and control polymer 5 (lacking amyloid-binding groups).

oligomers also exhibited enhanced binding to the SEVI amyloid putatively through multivalent binding.[21] Interestingly, while the binding of the BTA oligomers to SEVI dramatically increased compared to a monomeric BTA analogue (*e.g.*, by 590-fold in the case of a BTA pentamer), the improvement in the functional activity of these oligomers to reduce HIV infection was considerably less pronounced (*e.g.*, by only 65-fold in the case of a BTA pentamer).

From these previous results, we hypothesized that the improved effect of the BTA oligomers on reducing SEVI-mediated HIV infection could be a result of the increased size of the BTA oligomers compared to BTA monomers rather than their improved binding to SEVI. In order to test this hypothesis, here we investigated the effect of polymeric nanoparticles (NPs) containing covalently attached amyloid-binding compounds on SEVI-enhanced HIV infection (Figure 1). We designed these polymeric NPs to be approximately the same size as HIV virions[22] (~150 nm) to assess the effect of steric interferences on the reduction of SEVI enhanced HIV infection by an amyloid-binding agent. We found that these polymeric NPs had greatly (over 200-fold) increased potency in inhibiting SEVI-enhanced HIV infection in cells despite retaining similar (or slightly lower) binding properties to SEVI compared to an amyloid-binding monomer. The effects of these NPs on reduction of SEVI-mediated HIV infection were greater than the activity found for amyloid-binding oligomers with much stronger avidity. The results suggest that consideration of steric bulk in the design of SEVI-binding molecules could be an important factor along with thermodynamic binding for neutralizing the effects of natural, aggregated amyloid proteins on sexual transmission of HIV.

RESULTS AND DISCUSSION

Design, Synthesis, and Characterization of Polyacrylate-Based Polymers. Prior work has shown that polyacrylamide-based polymers carrying sialic acid groups could bind to influenza virus particles and effectively inhibit the direct binding of the virus to cells through steric inhibition.[23] Inspired by these previous studies, we hypothesized that amyloid-binding polymers or polymeric nanoparticles could create a significant steric barrier to block interactions between SEVI and HIV virions and, thus, effectively inhibit SEVI-mediated HIV infection. Here, we synthesized polyacrylate-based polymers carrying amyloid-binding BTA moieties. We chose to use polyacrylate-based polymers because they are nontoxic and synthetically accessible in useful quantities. Polyacrylate polymers are also known to form spherical nanoparticles of 100−200 nm in diameter,[24,25] which is approximately the same size as HIV virions.[22] Moreover, their capability to form nanoparticles of relatively narrow dispersity makes it possible to more accurately assess efficacy for reducing HIV infection compared to a mixture of polymers with large variability in size, shape, and aggregation state.

To develop a polyacrylate-based polymer carrying amyloid-binding BTA moieties, we synthesized an analogue of BTA-EG_6 (**1**, Figure 2)[16,19] comprising an acrylate group (**2**). This BTA-acrylate monomer **2** was then subjected to free-radical conditions[26,27] at

TABLE 1. Properties of Polyacrylate Polymers 3 and 5 and Nanoparticles Derived from Polymer 3

polymer	BTA incorporation (%)	M_n	M_w	PDI	apparent K_d to SEVI (μg/mL)	NP diameter DLS (nm)	NP PD DLS	NP diameter EM (nm)
amyloid binding polymer, **3**	56	68000	110000	1.63	14 $\pm$ 0.06	218	0.19	83
control polymer **5**	0	13000	18000	1.42	N/A	N/A	N/A	N/A

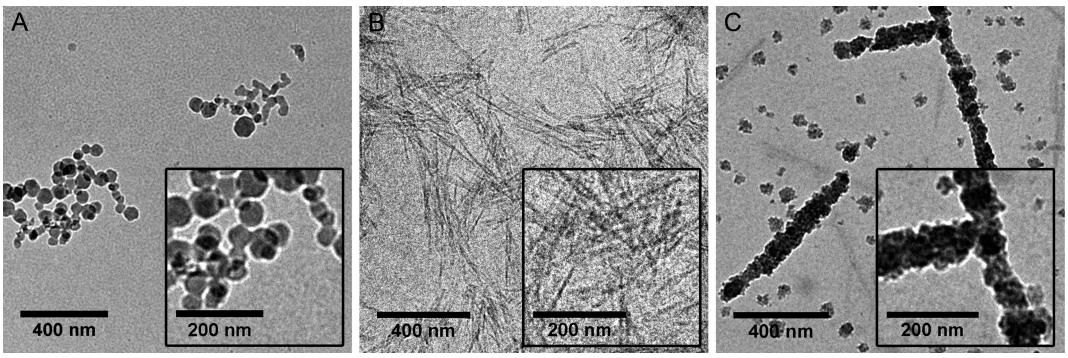

Figure 3. Representative Cryo-EM or non-Cryo TEM images of polymeric nanoparticles, SEVI fibrils, or a mixture of nanoparticles and SEVI fibrils: (A) cryo-EM images of polymeric nanoparticles carrying amyloid-binding BTA groups; (B) cryo-EM images of SEVI fibrils; (C) unstained TEM images of a sample containing SEVI fibrils and polymeric nanoparticles. The insets represent higher magnification images of the respective samples.

elevated temperature in the presence of acrylic acid and a catalytic amount of AIBN (radical initiator) to generate the polyacrylate polymer **3** (Figure 2). Analysis of polymer **3** by static light scattering−multiangle light scattering (SLS−MALS) revealed that this polymer had a number-average molecular weight (M_n) of 68K, with a polydispersity index (PDI) of 1.63 (Table 1). Examination of polymer **3** by ^{1}H NMR suggested that 56% of the residues in the polymer contained BTA groups.

As a control, we also synthesized polyacrylate-based polymer **5** (Figure 2) containing hexaethylene glycol groups but lacking the BTA moieties. This control polymer was designed to test whether amyloid-binding groups are necessary for reducing SEVI-mediated HIV infection. While this control polymer had a lower M_n and M_w than **3**, it had a similar PDI as the BTA-containing polyacrylate-based polymer **3** (Table 1).

Generation and Characterization of Polymeric Nanoparticles. The BTA-containing polyacrylate polymer **3** is substantially larger than the previously reported oligomers of BTA[21] and, thus, was expected to be useful to probe the effects of sterics on reducing SEVI-mediated HIV infection. However, the hydrophobic nature of **3** makes this polymer highly prone to uncontrolled aggregation in aqueous solutions. Formulation of polymer **3** into nanoparticles was, therefore, pursued with the goal of significantly narrowing the size and shape dispersity of aggregates, thereby making it easier to quantitatively assess the activity of these polymers in SEVI-mediated HIV infectivity assays.

In order to convert polymer **3** into nanoparticles, we used a previously reported solvent evaporation method[28,29] to generate spherical nanoparticles with average diameters of ~200 nm (PD = 0.19, see Figure S1 in the Supporting Information), as determined by dynamic light scattering (DLS). Analysis of these nanoparticles by cryo-electron microscopy (cryo-EM, Figure 3A) suggested a smaller average diameter of the spherical nanoparticles of 83 nm. Since larger particles tend to scatter more light than smaller particles, estimations of size of nanoparticles by DLS will often reflect a greater weight given to larger particles that may be present in the sample even if they represent only a minor fraction of particles.[30] Thus, we consider the estimation of nanoparticle diameter obtained from cryo-EM images as a more accurate method to determine the average size of nanoparticles in the sample. Regardless of the discrepancy in size of the nanoparticles as estimated by DLS or cryo-EM, spherical polymeric nanoparticles with diameters between 83 and 200 nm are of similar shape and size as HIV virions.[22]

We expected that nanoparticles in this size range should be large enough to impart significant steric interactions between virus particles and SEVI amyloid fibrils. When we incubated these particles with a solution of SEVI fibrils (Figure 3B), unstained transmission electron microscopy (TEM) images revealed a population of nanosized objects that were consistent with SEVI fibrils coated with nanoparticles (Figure 3C). The nanosized objects shown in Figure 3C were not present in samples containing nanoparticles (Figure 3A) or SEVI fibrils (Figure 3B) alone. These results from imaging, therefore, support that nanoparticles derived from polymer **3** can bind and coat SEVI fibrils and, thus, may be capable of sterically inhibiting interactions between SEVI and HIV virions.

Lastly, we evaluated the stability of the polymeric nanoparticles derived from polymer **3** by DLS. When incubated at 25 or 37 °C in deionized water, we

TABLE 2. Comparison of BTA-Containing Compounds

compound	apparent K_d (μM)	IC_{50} (μM)	IC_{50} normalized to $[BTA]_{tot}$ (μM)	ratio (K_d:IC_{50})
BTA-EG_6 Monomer (**1**)	0.127 $\pm$ 0.022[a]	13[c]	13	1:102
BTA-pentamer (**6**)	0.0004 $\pm$ 0.0002[b]	0.20[d]	1	1:500
polymer	0.206 $\pm$ 0.0009	0.21[d]	23	1:1
nanoparticle	N/A	0.059[d]	6	N/A

[a] For details, see ref 20. [b] For details, see ref 21. [c] IC_{50} values reflect reduction of SEVI-enhanced infection of HIV_{IIIB} in CEM-M7 cells. [d] IC_{50} values reflect reduction of SEVI-enhanced infection of HIV_{IIIB} in TZM-bl cells.

observed a slight decrease (<10%) in the average size of the particles over the first 6 h (at either temperature). Over a 48 h period, we observed a decrease in average particle size by ~18% at 25 °C and ~23% at 37 °C (see Figure S2 in the Supporting Information). The polydispersity (PD) of the nanoparticles, however, remained unchanged at either temperature over the 2-day period. For comparison, polymeric nanoparticles with poor stability have been characterized with large observed changes in size (by >30%) and PD (by >10-fold) over a period of less than a few hours.[31] Given that SEVI-mediated HIV infection in cells takes place within a 2 h period,[20,21] the nanoparticles derived from polymer **3** appear to have suitable stability for evaluation in infectivity assays.

Binding Studies of BTA-Containing Polyacrylate Polymer 3 and Control Polymer 5 with SEVI Fibrils. We quantified the interaction of polymer **3** and SEVI fibrils using a previously reported centrifugation method.[20,21] This assay revealed that polymer **3** bound to SEVI amyloid fibrils with an apparent K_d = 14 μg/mL (Table 1 and see Figure S3 in the Supporting Information). If we use the number-average molecular weight (M_n) as an estimate of the molecular weight (MW) of the polymer, the apparent K_d value is ~0.21 μM. For comparison, the reported K_d value for the binding of BTA-EG_6 to SEVI fibrils is 0.127 μM[20] (see also Table 2). We attribute this slightly weaker apparent K_d for polymer binding to SEVI compared to monomer to the likely possibility that the majority of the amyloid-binding BTA moieties are buried within the hydrophobic bulk of the polymer rather than remaining accessible to the aqueous environment and available for binding to an amyloid surface. While we expect nanoparticles to exhibit an apparent binding to SEVI that would be similar to polymer **3**, the centrifugation assay used in these studies could not be applied to measure apparent binding constants for the nanoparticles due to the colloidal nature of the nanoparticle suspensions (which results in pelleting of the nanoparticles upon centrifugation when either bound or unbound to SEVI).

In order to evaluate whether control polymer **5** (which lacks fluorescent amyloid-binding groups) exhibits any significant nonspecific binding to SEVI, we performed a competition assay where we incubated a constant concentration of 100 μg/mL of polymer **3** and 10 μg of SEVI amyloid fibrils in water in the presence of increasing concentrations of control polymer **5**. This competition assay made it possible to evaluate the binding between polymer **5** and SEVI by measuring the decrease in the fluorescence of polymer **3** if competitively displaced from the SEVI surface.[20,21] As expected, the results show that polymer **5** does not exhibit any significant binding to SEVI at concentrations $\leq$1 mg/mL (*i.e.*, at concentrations that were 10-fold higher than polymer **3**; see Figure S4 in the Supporting Information).

BTA-Containing Polymeric Nanoparticles Effectively Inhibit SEVI-Mediated HIV Infection. We measured the half-maximal inhibitory concentration (IC_{50}) of HIV infectivity with and without the presence of SEVI amyloid fibrils for our polyacrylate polymer **3** and our polymeric nanoparticles using a luciferase reporter cell line (TZM-bl cells[21]) that was exposed to infectious HIV_{IIIB}. For BTA-containing polyacrylate polymer **3**, we found an IC_{50} value of ~14 μg/mL (Figure 4A,B) for inhibition of SEVI-enhanced HIV infection. This IC_{50} value corresponds to a concentration of ~200 nM polymer, which is similar in activity to the previously reported most potent amyloid-targeting BTA-pentamer **6**[21] (Figure 5) for inhibiting SEVI-mediated infection of HIV. Additionally, polymer **3** was significantly more active on a per mole basis in this infection assay compared to BTA-EG_6 **1**.[20]

When we consider the activity of polymer **3** on a per BTA basis (IC_{50} = 23 μM), however, the polymers appeared to have activity similar to that of BTA-EG_6 **1** (IC_{50} = 13 μM). This lower than expected apparent activity for polymer **3** on a per BTA basis may be due to the heterogeneity of polymer aggregates that are likely formed in solution, resulting in a mixture of species with varying activity for binding to SEVI (and subsequent inhibition of SEVI-mediated HIV infection).

Interestingly, the BTA-containing polymeric nanoparticles exhibited an IC_{50} value of ~4 μg/mL (Figure 4 C,D), which corresponded to a concentration of 59 nM polymer. While the molar activity for these nanoparticles is the most active of any SEVI-binding species reported to date for reducing SEVI-enhanced HIV infection, the activity of these nanoparticles on a per BTA basis (IC_{50} = 6 μM) is also twice as active as BTA-EG_6[20] and over three times more active than polymer **3**. We attribute the increased activity of these nanoparticles relative to polymer **3** to the increased uniformity of shape and size of the nanoparticles compared to a complex mixture of aggregates that likely form with

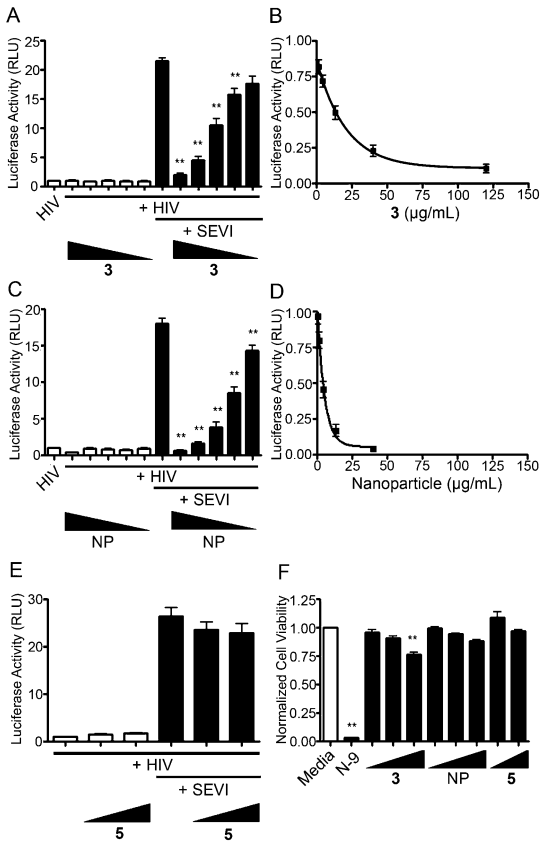

Figure 4. Representative graphs displaying the efficacy and toxicity of the polymers 3 and 5 as well as nanoparticles (NP) formulated from 3. (A) Graph showing the reduction of SEVI-mediated enhancement of HIV_{IIIB} infection in TZM-bl cells in the presence of polymer 3 at 1.5, 4.4, 13.3, 40, and 120 μg/mL as estimated by cellular luciferase expression levels normalized to HIV infectivity in the absence of both SEVI and polymer 3. (B) Dose−response curve of data shown in A normalized to HIV infectivity in the presence of SEVI only. Fitting the curve gives an IC_{50} value of 14 μg/mL, which is equivalent to 206 nM. (C) Graph showing reduction of SEVI-mediated enhancement of HIV_{IIIB} infection in TZM-bl cells in the presence of 1.5, 4.4, 13.3, 40, and 120 μg/mL BTA-containing nanoparticles (NPs) as estimated by cellular luciferase expression levels normalized to HIV infectivity in the absence of both SEVI amyloid fibrils and NPs. (D) Dose−response curve of data show in C normalized to HIV infectivity in the presence of SEVI only. Fitting the curve gives an IC_{50} value of 4 μg/mL, which is equivalent to 59 nM polymer. (E) Graph showing the reduction of SEVI-mediated enhancement of HIV_{IIIB} infection in TZM-bl cells in the presence of 40 and 120 μg/mL polymer 5 (negative control) as estimated by cellular luciferase expression levels normalized to HIV infectivity in the absence of both SEVI amyloid fibrils and polymer 5. (F) Graph showing the toxicity of polymers 3 and 5 and NPs in 3EC1 ectocervical cells as estimated by fluorescence of Alamar Blue normalized to cells alone. Polymer 3 and NPs dosed at 7.5, 30, and 120 μg/mL and control polymer 5 dosed at 40 and 120 μg/mL. These results show no statistically significant change in cell viability at concentrations of polymers 3 and 5 and NPs under 40 μg/mL. Statistical analysis by ANOVA with Turkey's post test. $^{**}p < 0.001$.

polymer **3** in aqueous solutions. The more narrow dispersity of shape and size of the nanoparticles presumably results in a higher concentration of polymeric aggregates with consistent activity for binding to SEVI.

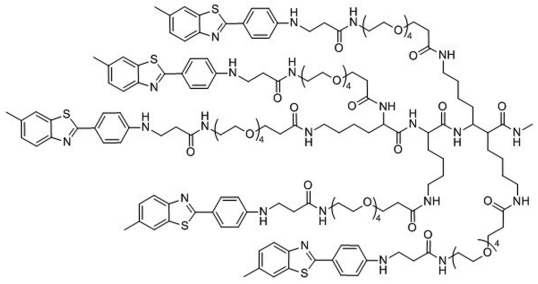

Figure 5. Structure of a previously reported BTA-pentamer 6[21]

The control polymer **5** was, as expected, completely ineffective at inhibiting SEVI-mediated HIV infection at concentrations below 40 μg/mL (~2 μM), emphasizing the importance of an amyloid-binding moiety on the polymer or nanoparticle for activity (Figure 4E).

In order to rule out that the observed activity of the polymers and nanoparticles reported here could be affected by unexpected toxicity of these materials to cells, we exposed ectocervical cells to high concentrations of **3**, **5**, and the BTA-containing polymeric nanoparticles for 24 h and measured cell viability using an Alamar Blue assay.[20] We found that none of the polymers or nanoparticles displayed significant toxicity at concentrations below 40 μg/mL (Figure 4F).

In order to evaluate the effect of sterics of SEVI-binding molecules on reduction of SEVI-mediated HIV infection, we compared the K_d values for binding to SEVI and IC_{50} values for inhibiting SEVI-enhanced HIV infection of BTA-EG_6 (monomer, **1**),[20] previously reported pentameric BTA molecule **6** (Figure 5),[21] and polymer **3**. Table 2 shows that the apparent K_d value of BTA-pentamer **6** to SEVI fibrils is >300-fold lower (*i.e.*, stronger) than the K_d value of BTA-EG_6 **1**. The IC_{50} value for reducing SEVI-enhanced HIV infection, however, was only 65-fold lower for pentamer **6** compared to monomer **1**. Comparing the ratio of K_d:IC_{50} for BTA-EG_6 monomer (~1:100) and BTA-pentamer (~1:500), therefore, illustrates that significantly reducing the apparent K_d of the SEVI-binding group is not accompanied by a corresponding strong reduction in SEVI-mediated HIV infection. For polymer **3**, the apparent K_d for binding to SEVI is slightly higher (*i.e.*, less tightly bound) than the monomer, but polymer **3** exhibits an IC_{50} that is 65-fold lower than monomer **1** for reducing SEVI-enhanced HIV infection. The ratio of K_d:IC_{50} for polymer **3** is thus approximately 1:1 (Table 2). This drastic increase in ratio of K_d:IC_{50} for polymer **3** compared to BTA-EG_6 monomer **1** or BTA-pentamer **6** suggests that the IC_{50} values are not well correlated with the apparent K_d values for binding to SEVI. The approximate 1:1 ratio of K_d:IC_{50} for polymer **3** suggests that the majority of polymer molecules that are bound to SEVI contribute to the inhibition of HIV infectivity enhanced by SEVI. In contrast, the monomeric- and pentameric-BTA compounds required a concentration for inhibiting

SEVI-mediated HIV infection that is at least 100-fold higher than the concentration required for binding to the amyloid surface. These observations suggest that steric bulk on the amyloid-binding agent greatly improves efficiency for inhibiting SEVI-mediated HIV infection.

CONCLUSION

In conclusion, we developed a polymer comprising amyloid-binding BTA moieties that maintained good affinity for SEVI amyloid fibrils. Nanoparticles generated from this polymer were similar in size and shape to HIV virions and effectively inhibited SEVI-mediated infectivity of HIV in cells. These polymers and nanoparticles were much more efficient at inhibiting SEVI-enhanced HIV infection compared to previously reported monomeric and pentameric versions of BTA, suggesting that steric hindrance can play a significant role in the design of effective SEVI neutralizing agents. These results further support the use of amyloid-targeting agents as prophylactic microbicide supplements for reducing HIV transmission through sexual contact. Since polymeric nanoparticles can be used as vehicles for controlled delivery of a variety of drugs,[29,32,33] the results reported here pave the way for development of multifunctional polymeric materials that can be targeted to amyloids associated with HIV transmission and possibly other diseases.[2,19,34,35]

METHODS

Synthesis of BTA-EG$_6$-acrylate (2). In a flame-dried round-bottom flask purged with N_2, BTA-EG$_6$ **1**[16] (500 mg, 0.99 mmol) was dissolved in 25 mL of dichloromethane (DCM). The reaction mixture was cooled to −78 °C in a dry ice bath (acetone/CO_2), and triethylamine was added (138 μL, 0.99 mmol) over 5 min. After incubation for an additional 5 min, a solution of acryloyl chloride (67 μL, 0.83 mmol) in DCM (1 mL) was added dropwise. After being warmed to room temperature (rt) over 24 h, the reaction mixture was concentrated to dryness and purified *via* silica gel chromatography using ethyl acetate (EtOAc) as the eluent. The product was dried under vacuum to afford an orange oil (334 mg, 72% yield). ^{1}H NMR (400 MHz, $CDCl_3$): δ 7.89 (3H, dd, *J* = 8.6, 10.1 Hz), 7.63 (1H, s), 7.23 (1H, d, *J* = 9 Hz), 6.66 (2H, d, *J* = 8.7 Hz), 6.40 (1H, dd, *J* = 1.9, 17 Hz), 6.11 (1H, dd, 10.1, 17 Hz), 5.82 (1H, dd, 1.9, 10 Hz), 4.30 (2H, t, *J* = 4.9 Hz), 3.67 (20H, m), 3.37 (2H, t, *J* = 4.7 Hz), 2.47 (3H, s). ^{13}C NMR (125 MHz, $CDCl_3$): 167.85, 166.31, 152.47, 150.63, 134.71, 134.40, 131.10, 129.00, 128.23, 127.62, 122.69, 121.90, 121.32, 112.67, 70.62, 70.60, 70.58, 70.57, 70.56, 70.33, 69.29, 69.10, 63.81, 43.17, 21.62. ESI-MS (*m/z*): calcd for $C_{29}H_{38}N_2O_7S$ $[M]^+$ 558.24, found $[M + H]^+$ 559.23.

Synthesis of Poly[acrylic acid-*co*-benzothiazole aniline hexa(ethylene glycol) acrylate] (3). Acrylic acid (32 μL, 0.47 mmol), **2** (263 mg, 0.47 mmol), and AIBN (4 mg, 0.024 mmol) were dissolved in butyl acetate (1 mL). The reaction mixture was degassed by gently bubbling dry N_2 gas with stirring for 30 min. After degassing, the reaction vial was sealed under N_2 atmosphere and placed in an oil bath at 65 °C for 16 h. After being cooled to rt, the cloudy solution was placed in a 50 mL conical vial. The reaction vial was rinsed with DCM (2 mL) and added to the conical vial. The polymer was precipitated by addition of hexanes (30 mL), and the solution was decanted. The polymer was redissolved in DCM and again precipitated with hexanes. The product was dried under vacuum to afford a yellow solid (100 mg, 34% yield). ^{1}H NMR (400 MHz, $CDCl_3$): δ 7.82 (3H, bs), 7.56 (1H, bs), 7.21 (1H, bs), 6.62 (2H, bs), 4.16 (2H, bs), 3.29 (20H, bs), 2.42 (3H, bs), 1.97 (1H, bs), 1.69 (2H, bs). Integration of aromatic protons in the region δ 6.62−7.82 ppm was used to determine incorporation of monomer **2** (see the Supporting Information for details).

Synthesis of Hexaethylene Glycol Monomethyl Ether Acrylate (4). In a flame-dried round-bottom flask purged with N_2 was dissolved hexaethylene glycol monomethyl ether (304 mg, 1.03 mmol) in DCM (5 mL). The reaction mixture was cooled to −78 °C in a dry ice bath (acetone/CO_2), and triethylamine was added (172 μL, 1.23 mmol) over 5 min. After another 5 min, a solution of acryloyl chloride (100 μL, 1.23 mmol) in DCM (1 mL) was added dropwise. After being warmed to rt over 24 h, the reaction mixture was concentrated to dryness and purified *via* silica gel chromatography using EtOAc as the eluent. The product was dried under vacuum to afford an orange oil (200 mg, 56% yield). ^{1}H NMR (500 MHz, $CDCl_3$): δ 6.43 (1H, dd, *J* = 1.4, 17.4 Hz), 6.15 (1H, dd, *J* = 10.4, 17.3 Hz), 5.84 (1H, dd, *J* = 1.4, 10.4 Hz), 4.31 (2H, t, *J* = 5.3 Hz), 3.74 (2H, t, *J* = 5 Hz), 3.65 (18H, m), 3.54 (2H, t, 4.5 Hz), 3.37 (3H, s). ^{13}C NMR (125 MHz, $CDCl_3$): δ 166.33, 131.23, 128.37, 72.03, 70.73, 70.68, 70.63, 69.24, 63.84, 59.19. ESI-MS (*m/z*): calcd for $C_{16}H_{30}O_8$ $[M]^+$ 350.19, found $[M + H]^+$ 351.33, $[M + NH_4]^+$ 368.32 and $[M + Na]^+$ 373.36.

Synthesis of Poly(hexaethylene glycol monomethyl ether acrylate) (5). Compound **6** (180 mg, 0.51 mmol) and AIBN (2 mg, 0.013 mmol) were dissolved in butyl acetate (1 mL). The reaction mixture was degassed by gently bubbling dry N_2 gas with stirring for 30 min. After degassing, the reaction vial was sealed under N_2 atmosphere and placed in an oil bath at 65 °C for 16 h. After being cooled to room temperature, the cloudy solution was placed in a 50 mL conical vial. The reaction vial was rinsed with DCM (2 mL) and added to the conical vial. The polymer was precipitated by addition of hexanes (30 mL), and the solution was decanted. The polymer was redissolved in DCM and again precipitated with hexanes. The product was dried under vacuum to afford a colorless oil. ^{1}H NMR (400 MHz, $CDCl_3$): δ 4.17 (2H, bs), 3.68 (22H, bm), 3.38 (3H, bs), 2.31 (1H, bs), 1.78 (2H, bs), 1.62 (1H, bs).

Polymer Analysis. Polymer polydispersity index (PDI) and molecular weight were determined by size-exclusion chromatography (Phenomenex Phenogel 5u **10**, 1K - 75K, 300 × 7.80 mm in series with a Phenomenex Phenogel 5u **10**, 10−1000 K, 300 × 7.80 mm (0.05 M LiBr in DMF, 0.75 mL/min, 60 °C)) using a Shimadzu LA-10AT pump equipped with a UV detector (Hitachi-Elite LaChrom L-2420), a multiangle light scattering detector (DAWN-HELEOS, Wyatt Technology), and a refractive index detector (Hitachi L-2490). Data analysis was performed using the ASTRA software package.

Nanoparticle Formulation. We dissolved 2 mg of polymer **3** in 2 mL of tetrahydrofuran (THF). This solution was added dropwise to an equal volume of deionized (DI) water with vigorous stirring. After the solution was stirred for 30 min, the THF was removed *in vacuo* and the remaining 1 mg/mL nanoparticle solution was analyzed *via* dynamic light scattering.

Nanoparticle Analysis by Dynamic Light Scattering. Particle size determination by dynamic light scattering was performed on a Wyatt DynaPro NanoStar (Wyatt Technology, Santa Barbara, CA) instrument using a disposable cuvette (Eppendorf UVette 220−1600 nm). Samples were analyzed using a concentration of nanoparticles of 1 mg/mL (with respect to polymer concentration) and data processed using Wyatt DYNAMICS V7 software. Data were exported for final plotting using GraphPad Prism 5 (GraphPad Software, Inc., La Jolla, CA), and a representative plot of signal intensity *versus* radius is shown in Figure S1 (Supporting Information).

Nanoparticle and SEVI Analysis by Cryo-EM. Nanoparticles were resuspended in a volume (50 μL) of water with a concentration of 20 mg/mL nanoparticle (with respect to polymer

concentration) prior to imaging. For SEVI, the amyloid fibrils were suspended at a concentration of 10 mg/mL (with respect to peptide concentration) in PBS. Small aliquots (<5 μL) of each sample were separately applied to holey grids, which had been glow discharged and plasma cleaned. These Cryo-EM samples were vitrified using liquid ethane as the cryogen. Frozen samples were transferred into a precooled cryo-transfer holder to maintain low temperature. Images acquired on a FEI Tecnai G2 Sphera operated at 200 keV using a Gatan Ultrascan 1000 UHS 4 MP CCD camera.

Preparation of SEVI Fibrils. PAP248-286 was dissolved in PBS at a concentration of 10 mg/mL. Fibrils were formed by agitation in an Eppendorf Thermomixer at 1400 rpm and 37 °C for 72 h. The presence of fibrils was confirmed by a previously described Congo Red spectroscopic assay.[21,36]

TEM Imaging of SEVI Fibrils Incubated with Nanoparticles. In order to obtain TEM images of SEVI fibrils incubated with NP, a 5 μL solution of NPs (5 mg/mL) was incubated with a 2 μL solution of SEVI (2 mg/mL) in water over an air plasma oxidized EM grid. The mixture was agitated *via* pipet on the grid for approximately 5 min. After 5 min, excess water was wicked away using filter paper, and the dried sample was subjected to TEM imaging on a FEI Tecnai G2 Sphera using a Gatan Ultrascan 1000 UHS 4 MP CCD camera.

Measurement of the Apparent Dissociation Constant, K_d, of 3 to SEVI Fibrils. The binding of polymer **3** to SEVI amyloid fibrils was estimated using a centrifugation assay described previously.[20,21] Briefly, 200 μL of various concentrations of **3** in 5% DMSO/water were incubated in the presence or absence of 10 μg of SEVI to give a final volume of 201 μL of solution. These incubations were performed in duplicate runs and allowed to equilibrate for 12 h at room temperature. After equilibration, each solution was centrifuged at 16000*g* for 30 min at 4 °C. The supernatants were separated from the pelleted fibrils, and 200 μL of fresh water was added to resuspend the pellets. Aliquots (100 μL) of each resuspended pellet were pipetted into a cuvette (ultra-microcuvette,10 mm light path, Hellma, Müllheim, Germany), and the fluorescence of the bound molecule was determined at 355 nm excitation and 420 nm emission using a spectrofluorometer (Photon Technology International, Inc., Birmingham, NJ). Each measurement experiment was repeated at least 3 times. Error bars represent standard deviations from the mean. The graph shown in Figure S3 (Supporting Information) shows the fluorescence intensity versus concentration of polymer **3**; the data were fitted using the following one-site specific binding algorithm to determine K_d: $Y = B_{max}X/(K_d + X)$, where X is the concentration of **3**, Y is the specific binding fluorescence intensity, and B_{max} corresponds to the apparent maximal observable fluorescence upon binding of BTA polymer to SEVI fibrils. The data were processed using GraphPad Prism 5 (GraphPad Software, Inc., La Jolla, CA).

Evaluation of SEVI-Mediated Enhancement of HIV-1 Infectivity of TZM-bl Cells in the Presence of BTA Polymer and Nanoparticles. TZM-bl cells (in DMEM culture medium supplemented with 10% FBS, 50 units/mL penicillin, and 50 μg/mL streptomycin) were seeded on 96-well flat-bottomed tissue culture plates at a density of 4×10^3 cells/well. Plates were incubated for 12 h (in a humidified atmosphere of 95% air, 5% CO2 at 37 °C) to promote attachment of cells to the wells. HIV_{IIIB} virions were then pretreated for 10 min at room temperature with 15 μg/mL SEVI fibrils in the presence or absence of polymer **3**, **5**, or polymeric nanoparticle. Treated virions were then added to the plated TZM-bl cells and were incubated for 2 h at 37 °C. After incubation, the cells were washed with DPB, and the media was replaced. Infection was assayed after 72 h by quantifying luciferase expression with PerkinElmer Britelite Plus and measuring luminescence with a microplate reader (DTX880, Beckman Coulter). All data are represented as the mean ± standard deviation of triplicate measurements. ANOVA with Tukey's post test was employed in all analyses of data. A p-value <0.05 was considered statistically significant.

Toxicity Assay. Cervical epithelial (ectocervical) cells (3EC1 cell line) were treated for 24 h with polymer **3**, polymeric nanoparticles, and polymer **5** at concentrations up to 40 μg/mL. After 24 h, cell viability was analyzed by measuring cellular metabolic activity using the resazurin cytotoxicity assay (Alamar Blue; Invitrogen), in accordance with the manufacturer's protocol. Cells were also treated with 0.1% Nonoxynol-9 as a positive control for cytotoxicity.

Conflict of Interest: The authors declare no competing financial interest.

Acknowledgment. This work was supported, in part, by NIH Grant Nos. R21AI094511 and R33AI094511, a California HIV/AIDS Research Program grant (ID10-SD-034), and by the University of Rochester Center for AIDS Research (NIH P30AI078498). We also acknowledge the NIH for support of the mass spectrometry facility at UCSD (S10RR25636). We gratefully acknowledge Dr. Joseph Patterson, Dr. Matthew Thompson, Kate Veccharelli, and Prof. Nathan Gianneschi for help with characterization of polymers and nanoparticles.

Supporting Information Available: Additional experimental details and characterization of molecules. This material is available free of charge *via* the Internet at http://pubs.acs.org/.

REFERENCES AND NOTES

1. Royce, R. A.; Sena, A.; Cates, W., Jr.; Cohen, M. S. Sexual Transmission of HIV. *N. Engl. J. Med.* **1997**, *336*, 1072–1078.
2. Münch, J.; Rücker, E.; Ständker, L.; Adermann, K.; Goffinet, C.; Schindler, M.; Wildum, S.; Chinnadurai, R.; Rajan, D.; Specht, A.; et al. Semen-Derived Amyloid Fibrils Drastically Enhance HIV Infection. *Cell* **2007**, *131*, 1059–1071.
3. Roan, N. R.; Müller, J. A.; Liu, H.; Chu, S.; Arnold, F.; Stürzel, C. M.; Walther, P.; Dong, M.; Witkowska, H. E.; Kirchhoff, F.; et al. Peptides Released by Physiological Cleavage of Semen Coagulum Proteins Form Amyloids That Enhance HIV Infection. *Cell Host Microbe* **2011**, *10*, 541–550.
4. Arnold, F.; Schnell, J.; Zirafi, O.; Stürzel, C.; Meier, C.; Weil, T.; Ständker, L.; Forssmann, W.-G.; Roan, N. R.; Greene, W. C.; et al. Naturally Occurring Fragments from Two Distinct Regions of the Prostatic Acid Phosphatase Form Amyloidogenic Enhancers of HIV Infection. *J. Virol.* **2012**, *86*, 1244–1249.
5. Roan, N. R.; Münch, J.; Arhel, N.; Mothes, W.; Neidleman, J.; Kobayashi, A.; Smith-McCune, K.; Kirchhoff, F.; Greene, W. C. The Cationic Properties of SEVI Underlie Its Ability to Enhance Human Immunodeficiency Virus Infection. *J. Virol.* **2009**, *83*, 73–80.
6. Münch, J.; Sauermann, U.; Yolamanova, M.; Raue, K.; Stahl-Hennig, C.; Kirchhoff, F. Effect of Semen and Seminal Amyloid on Vaginal Transmission of Simian Immunodeficiency Virus. *Retrovirology* **2013**, *10*, 148.
7. Easterhoff, D.; DiMaio, J. T. M.; Doran, T. M.; Dewhurst, S.; Nilsson, B. L. Enhancement of HIV-1 Infectivity by Simple, Self-Assembling Modular Peptides. *Biophys. J.* **2011**, *100*, 1325–1334.
8. Castellano, L. M.; Shorter, J. The Surprising Role of Amyloid Fibrils in HIV Infection. *Biology.* **2012**, *1*, 58–80.
9. Roan, N. R.; Sowinski, S.; Münch, J.; Kirchhoff, F.; Greene, W. C. Aminoquinoline Surfen Inhibits the Action of SEVI (Semen-Derived Enhancer of Viral Infection). *J. Biol. Chem.* **2010**, *285*, 1861–1869.
10. Hauber, I.; Hohenberg, H.; Holstermann, B.; Hunstein, W.; Hauber, J. The Main Green Tea Polyphenol Epigallocatechin-3-Gallate Counteracts Semen-Mediated Enhancement of HIV Infection. *Proc. Natl. Acad. Sci. U.S.A.* **2009**, *106*, 9033–9038.
11. Popovych, N.; Brender, J. R.; Soong, R.; Vivekanandan, S.; Hartman, K.; Basrur, V.; Macdonald, P. M.; Ramamoorthy, A. Site Specific Interaction of the Polyphenol EGCG with the SEVI Amyloid Precursor Peptide PAP(248−286). *J. Phys. Chem. B* **2012**, *116*, 3650–3658.
12. Hartjen, P.; Frerk, S.; Hauber, I.; Matzat, V.; Thomssen, A.; Holstermann, B.; Hohenberg, H.; Schulze, W.; Schulze Zur Wiesch, J.; van Lunzen, J. Assessment of the Range of the HIV-1 Infectivity Enhancing Effect of Individual Human Semen Specimen and the Range of Inhibition by EGCG. *AIDS Res. Ther.* **2012**, *9*, 2.

13. Sheftic, S. R.; Snell, J. M.; Jha, S.; Alexandrescu, A. T. Inhibition of Semen-Derived Enhancer of Virus Infection (SEVI) Fibrillogenesis by Zinc and Copper. *Eur. Biophys. J.* **2012**, *41*, 695–704.
14. Kirchhoff, F.; Munch, J. Blocking Semen-Mediated Enhancement of HIV Infection by Amyloid-Binding Small Molecules. *Future Virol.* **2011**, *6*, 183–186.
15. Inbar, P.; Yang, J. Inhibiting Protein-Amyloid Interactions with Small Molecules: A Surface Chemistry Approach. *Bioorg. Med. Chem. Lett.* **2006**, *16*, 1076–1079.
16. Inbar, P.; Li, C. Q.; Takayama, S. A.; Bautista, M. R.; Yang, J. Oligo(ethylene glycol) Derivatives of Thioflavin T as Inhibitors of Protein-Amyloid Interactions. *ChemBioChem* **2006**, *7*, 1563–1566.
17. Inbar, P.; Bautista, M. R.; Takayama, S. A.; Yang, J. Assay To Screen for Molecules That Associate with Alzheimer's Related β-Amyloid Fibrils. *Anal. Chem.* **2008**, *80*, 3502–3506.
18. Capule, C. C.; Yang, J. Enzyme-Linked Immunosorbent Assay-Based Method to Quantify the Association of Small Molecules with Aggregated Amyloid Peptides. *Anal. Chem.* **2012**, *84*, 1786–1791.
19. Habib, L. K.; Lee, M. T. C.; Yang, J. Inhibitors of Catalase-Amyloid Interactions Protect Cells from Beta-Amyloid-Induced Oxidative Stress and Toxicity. *J. Biol. Chem.* **2010**, *285*, 38933–38943.
20. Olsen, J. S.; Brown, C.; Capule, C. C.; Rubinshtein, M.; Doran, T. M.; Srivastava, R. K.; Feng, C.; Nilsson, B. L.; Yang, J.; Dewhurst, S. Amyloid-Binding Small Molecules Efficiently Block SEVI (Semen-Derived Enhancer of Virus Infection)- and Semen-Mediated Enhancement of HIV-1 Infection. *J. Biol. Chem.* **2010**, *285*, 35488–35496.
21. Capule, C. C.; Brown, C.; Olsen, J. S.; Dewhurst, S.; Yang, J. Oligovalent Amyloid-Binding Agents Reduce SEVI-Mediated Enhancement of HIV-1 Infection. *J. Am. Chem. Soc.* **2012**, *134*, 905–908.
22. Briggs, J. A. G.; Wilk, T.; Welker, R.; Kra, H.-G.; Fuller, S. D. Structural Organization of Authentic, Mature HIV-1 Virions and Cores. *EMBO J.* **2003**, *22*, 1707–1715.
23. Sigal, G. B.; Mammen, M.; Dahmann, G.; Whitesides, G. M. Polyacrylamides Bearing Pendant α-Sialoside Groups Strongly Inhibit Agglutination of Erythrocytes by Influenza Virus: The Strong Inhibition Reflects Enhanced Binding through Cooperative Polyvalent Interactions. *J. Am. Chem. Soc.* **1996**, *118*, 3789–3800.
24. Chouinard, F.; Buczkowski, S.; Lenaerts, V. Poly-(Alkylcyanoacrylate) Nanocapsules: Physicochemical Characterization and Mechanism of Formation. *Pharm. Res.* **1994**, *11*, 869–874.
25. Anton, N.; Benoit, J.-P.; Saulnier, P. Design and Production of Nanoparticles Formulated from Nano-Emulsion Templates-A Review. *J. Controlled Release* **2008**, *128*, 185–199.
26. Arias, C.; Lopez-Gonzalez, M. C.; Fernandez-Garcia, M.; Barrales-Rienda, J. M.; Madruga, E. L. Free-Radical Copolymerization of Methyl Acrylate with Methyl Methacrylate in Benzene Solution. *Polymer* **1993**, *34*, 1786–1789.
27. Dube, M. A.; Rilling, K.; Penlidis, A. A Kinetic Investigation of Butyl Acrylate Polymerization. *J. Appl. Polym. Sci.* **1991**, *43*, 2137–2145.
28. Yan, C.; Yuan, X.; Kang, C.; Zhao, Y.-H.; Liu, J.; Guo, Y.; Lu, J.; Pu, P.; Sheng, J. Preparation of Carmustine-loaded PLA Ultrasmall-nanoparticles by Adjusting Micellar Behavior of Surfactants. *J. Appl. Polym. Sci.* **2008**, *110*, 2446–2452.
29. Farokhzad, O. C.; Cheng, J.; Teply, B. A.; Sherifi, I.; Jon, S.; Kantoff, P. W.; Richie, J. P.; Langer, R. Targeted Nanoparticle-Aptamer Bioconjugates for Cancer Chemotherapy in Vivo. *Proc. Natl. Acad. Sci. U.S.A.* **2006**, *103*, 6315–6320.
30. Hoo, C. M.; Starostin, N.; West, P.; Mecartney, M. L. A Comparison of Atomic Force Microscopy (AFM) and Dynamic Light Scattering (DLS) Methods to Characterize Nanoparticle Size Distributions. *J. Nanoparticle Res.* **2008**, *10*, 89–96.
31. Muller, R. H.; Lherm, C.; Herbort, J.; Blunk, T.; Couvreur, P. Alkylcyanoacrylate Drug Carriers: I. Physicochemical Characterization of Nanoparticles with Different Alkyl Chain Length. *Int. J. Pharm.* **1992**, *84*, 1–11.
32. Ungaro, F.; d'Angelo, I.; Coletta, C.; d'Emmanuele di Villa Bianca, R.; Sorrentino, R.; Perfetto, B.; Tufano, M. A.; Miro, A.; La Rotonda, M. I.; Quaglia, F. Dry Powders Based on PLGA Nanoparticles for Pulmonary Delivery of Antibiotics: Modulation of Encapsulation Efficiency, Release Rate and Lung Deposition Pattern by Hydrophilic Polymers. *J. Controlled Release* **2012**, *157*, 149–159.
33. De Gracia Lux, C.; Joshi-Barr, S.; Nguyen, T.; Mahmoud, E.; Schopf, E.; Fomina, N.; Almutairi, A. Biocompatible Polymeric Nanoparticles Degrade and Release Cargo in Response to Biologically Relevant Levels of Hydrogen Peroxide. *J. Am. Chem. Soc.* **2012**, *134*, 15758–15764.
34. Romero, D.; Sanabria-Valentín, E.; Vlamakis, H.; Kolter, R. Biofilm Inhibitors That Target Amyloid Proteins. *Chem. Biol.* **2013**, *20*, 102–110.
35. Agyare, E.; Kandimalla, K. Delivery of Polymeric Nanoparticles to Target Vascular Diseases. *Biomol. Res. Ther.* **2014**, *S1:001*, 1–11.
36. Nilsson, M. R. Techniques to Study Amyloid Fibril Formation in Vitro. *Methods* **2004**, *34*, 151–160.